Ab Initio and Semiempirical Calculations of Geometry and Electronic Spectra of Ruthenium Organic Complexes and Modeling of Spectroscopic Changes upon DNA Binding

Anders Broo* and Per Lincoln

Department of Physical Chemistry, Chalmers University of Technology, 412 96 Göteborg, Sweden

Received October 1, 1996[⊗]

A new parameter set for the INDO model is proposed for ruthenium as well as a general way to obtain parameters for any transition metal. The ionic state of the transition metal rather than the atomic state has been used to obtain ionization potentials. A rather large series of ruthenium complexes are treated in this work, ranging from $[Ru(NH_3)_6]^{2+}$ to $[Ru(phen)_2dppz]^{2+}$ (phen = phenanthroline, dppz = dipyrido[3,2-*a*:2′,3′-*c*]phenazine) and the so-called Creuz−Taube ion ($[Ru(NH_3)_5$-pyrazine-$Ru(NH_3)_5]^{4+/5+}$). In all the complexes, Ru has a formal oxidation state of 2+ or 3+. Geometry optimizations at both ab initio and semiempirical INDO levels are presented. The proposed parametrization of the INDO model reproduces both the geometry and the absorption spectra of ruthenium complexes with good accuracy. Bond length changes upon changing the oxidation state of the metal are not fully reproduced. The ab initio calculations predict Ru−N bond lengths that are 0.1−0.15 Å too long compared to observations. The corresponding bond lengths are calculated in better agreement with observations with the INDO model. The effect upon DNA binding on the calculated spectrum of the $[Ru(phen)_2dppz]^{2+}$ complex was investigated. The DNA binding was modeled by a molecular mechanics energy minimization of a $[Ru(phen)_2dppz]^{2+}$−poly(dA-dT) complex.

Introduction

Ruthenium complexes, especially $[Ru(bpy)_3]^{2+}$, are among the most experimentally studied organometallic complexes, due to their unique combination of chemical stability, redox properties, electron and energy transfer properties, and excited state reactivity.[1] Few quantum chemical investigations of ruthenium complexes have been published.[2−4] This list of computational work on ruthenium complexes is certainly not complete, and many works have probably escaped our attention. Until recently, only semiempirical methods[2,4a] and density functional theory methods[3] have been used. Part of the problem in applying ab initio quantum chemical methods to second-row transition metals is the relatively large size, in terms of basis functions, of the metal complexes. Another aspect is the importance of relativistic effects on the electron structure of the metal, which is not properly accounted for in a traditional Hartree−Fock calculation. Yet another important factor is the so far unclear role of electron correlation on geometry and binding energy of second-row transition metals.[5] However, attempts have been made to clarify the effect of electron correlation on the geometry of second-row organometallic complexes.[6] An alternative to ab initio calculations on these complicated systems are semiempirical methods, which also have been used in the past. Among the most popular semiempirical methods, MNDO, AM1, PM3, CNDO, SINDO, and INDO, only the CNDO- and the INDO-based methods can handle transition metals.[7] However, transition metals, especially second-row transition metals, have not been carefully parametrized to reproduce both geometry and absorption spectra so far. In this work, we propose a parametrization for ruthenium using the INDO model Hamiltonian.[8] For this parametrization, we have selected a number of ruthenium complexes with different bonding properties (see Chart 1).

The simplest complex is the $[Ru(NH_3)_6]^{2+}$ cation, where the metal−ligand bond is of σ type. In $[Ru(bpy)_3]^{2+}$, both σ and π type bonding occurs. The Ru−N bonds in $[Ru(bpy)_3]^{2+}$ are shorter than the Ru−NH_3 bonds, which indicates a significant backbonding between the Ru t_{2g} orbitals and the π^* orbitals of the bipyridines. The geometries of these complexes have been determined by X-ray crystallography,[8,9] and the absorption spectra are known and fully understood.[10,11] We have also calculated the geometry of some ruthenium−water complexes

[⊗] Abstract published in *Advance ACS Abstracts,* May 1, 1997.

(1) Juris, A.; Balzani, V.; Barigelletti, F.; Campagna, S.; Belser, P.; von Zelewsky, A. *Coord. Chem. Rev.* **1988**, *84*, 85.

(2) (a) Larsson, S.; Broo, A.; Källebring, B.; Volosov, A. *Int. J. Quantum Chem., Quantum Biol. Symp.* **1988**, *15*, 1. (b) Broo, A.; Larsson, S. *Int. J. Quantum Chem., Quantum Biol. Symp.* **1989**, *16*, 185. (c) Reimers, J. R.; Hush, N. S. *J. Chem. Phys.* **1991**, *95*, 9773. (d) Zeng, J.; Hush, N. S.; Reimers, J. R. *J. Chem. Phys.* **1995**, *99*, 10459. (e) Stavrev, K. K.; Zerner, M. C.; Meyer, T. J. *J. Am. Chem. Soc.* **1995**, *117*, 8684. (f) Woitellier, S.; Launay, J. P.; Joachim, C. *Chem. Phys.* **1989**, *131*, 481. (g) Joachim, C.; Launay, J. P.; Woitellier, S. *Chem. Phys.* **1990**, *147*, 131. (h) Joachim, C.; Launay, J. P. *J. Mol. Electron* **1990**, *6*, 37.

(3) (a) Lauher, J. W. *Inorg. Chim. Acta* **1980**, *39*, 119. (b) Ondrechen, M. J.; Ratner, M. A.; Ellis, D. E. *J. Am. Chem. Soc.* **1981**, *103*, 1656. (c) Ondrechen, M. J.; Ellis, D. E.; Ratner, M. A. *Chem. Phys. Lett.* **1984**, *109*, 50. (d) Zhang, L.-T.; Ko, J.; Ondrechen, M. J. *J. Am. Chem. Soc.* **1987**, *109*, 1666.

(4) (a) Broo, A.; Larsson, S. *Chem. Phys.* **1992**, *161*, 363. (b) Newton, M. D. *J. Phys. Chem.* **1988**, *92*, 3049. (c) Newton, M. D. *J. Phys. Chem.* **1986**, *90*, 3734. (d) Itagaki, H.; Koga, N.; Morokuma, K.; Saito, Y. *Organometallics* **1993**, *12*, 1648. (e) Riehl, J.-F.; Koga, N.; Morokuma, K. *J. Am. Chem. Soc.* **1994**, *116*, 5414. (f) Wakatsuki, Y.; Koga, N.; Yamazaki, H.; Morokuma, K. *J. Am. Chem. Soc.* **1994**, *116*, 8105. (g) Siegbahn, P. E. M. *J. Phys. Chem.* **1995**, *99*, 12723. (h) Åkesson, R.; Petterson, L. G. M.; Sandström, M.; Wahlgren, U. *J. Am. Chem. Soc.* **1994**, *116*, 8691.

(5) Veillard, A. *Chem. Rev.* **1991**, *91*, 743.

(6) Siegbahn, P. E. M.; Svensson, M. *Chem. Phys. Lett.* **1993**, *216*, 147.

(7) (a) MNDO: Dewar, M. J. S.; Thiel, W. *J. Am. Chem. Soc.* **1977**, *99*, 4899. (b) AM1: Dewar, M. J. S.; Zoebisch, E. G.; Healy, E. F.; Stewart, J. J. P. *J. Am. Chem. Soc.* **1985**, *107*, 3902. (c) PM3: Stewart, J. J. P. *J. Comput. Chem.* **1989**, *2*, 209. (d) CNDO: Pople, J. A.; Santry, D. P.; Segal, G. A. *J. Chem. Phys.* **1965**, *43*, S129. (e) SINDO: Jug, K.; Nanda, D. N. *Theor. Chim. Acta* **1980**, *57*, 95. (f) INDO: Ridley, J. E.; Zerner, M. C. *Theor. Chim. Acta* **1973**, *32*, 111; **1976**, *42*, 223. (g) Bacon, A. D.; Zerner, M. C. *Theor. Chim. Acta* **1979**, *53*, 21. (h) Pople, J. A.; Beveridge, D. L.; Dobosh, P. A. *J. Chem. Phys.* **1967**, *47*, 2026.

(8) Stynes, H.; Ibers, J. A. *Inorg. Chem.* **1971**, *10*, 2304.

(9) Rillema, D. P.; Jones, D. S.; Levy, H. *J. Chem. Soc., Chem. Commun.* **1979**, 849.

S0020-1669(96)01193-7 CCC: $14.00

Chart 1

I $[Ru(NH_3)_6]^{2+/3+}$ **II** $[Ru(bpy)_3]^{2+}$ **III** $[Ru(NH_3)_5\text{-}pyz]^{2+}$

IV $[Ru(NH_3)_5\text{-}py]^{2+}$ **V** $[Ru(NH_3)_5\text{-}pyz\text{-}Ru(NH_3)_5]^{4+/5+}$ **VI** $[Ru(py)_6]^{2+}$

VII $[Ru(phen)_3]^{2+}$ **VIII** $[Ru(phen)_2dppz]^{2+}$ **IX** $[Ru(bpy)_2(py)_2]^{2+}$ (trans)

X $[Ru(phen)_2biquin]^{2+}$ **XI** $[Ru(H_2O)_6]^{2+/3+}$ **XII** $[Ru(bpy)_2(OH)(H_2O)]^{2+}$

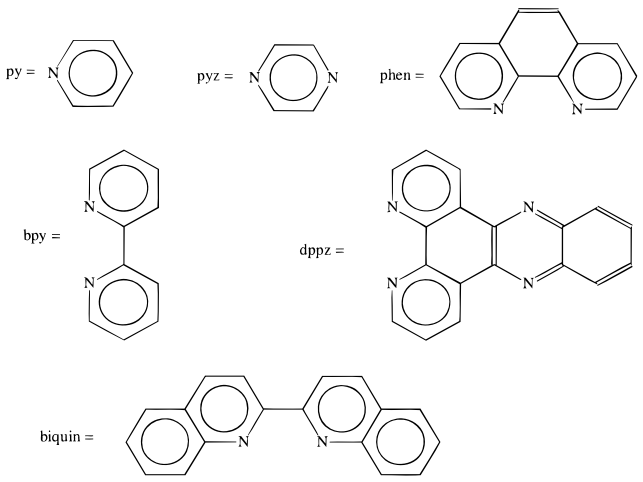

in order to test the generality of the proposed parametrization. Only a few ruthenium complexes have been used in the training set for the parameter determination. If, then, a larger set of metal complexes are well described regarding geometry and absorption spectra using these parameters, the parametrization has a good chance to be as general as ever possible.

In addition to the semiempirical calculations, we have performed ab initio geometry optimizations of $[Ru(NH_3)_6]^{2+}$ and $[Ru(phen)_3]^{2+}$ for reference purposes.

Computational Details

In all the ruthenium complexes, the ligand field around the central ruthenium ion has nearly octahedral (O_h) symmetry. The ruthenium ion has either a $4d^6$ electron configuration, Ru(II), or a $4d^5$ electron configuration, Ru(III). Three d orbitals, *xz*, *yz*, and *xy*, are occupied, and two, x^2-y^2 and z^2, are unoccupied. In a perfect O_h ligand field, the occupied d orbitals are degenerate and have t_{2g} symmetry, and the unoccupied d orbitals are also degenerate and have e_g symmetry. When the perfect O_h symmetry is broken by the ligands, the occupied d orbitals, as well as the two unoccupied metal orbitals, will not remain degenerate but will rather be separated in energy. All the Ru(II) complexes are assumed to have low-spin d^6 metal configuration, since the amine group and the nitrogen heterocycles are known to produce a rather large ligand field.[12] The Ru(III) complexes are assumed to have a low-spin d^5 metal configuration, which is also observed in most Ru(III) complexes for the same reason.

The ab initio geometry optimizations were performed with the GAMESS program.[13] The Ru ions were described using the relativistic effective core potential of Stevens et al., which includes 28 core electrons and the associated valence double-ζ basis set.[14] The basis set for the other atoms was either the minimal basis set STO-3G or the split valence 6-31G basis set.[15] The two basis sets are abbreviated as SBK+STO-3G and SBK+6-31G, respectively. The semiempirical calculations, both geometry (INDO/1) and absorption spectra (INDO/S), were performed with the ZINDO program package.[16] Solvent effects on absorption spectra were estimated by using the self-consistent reaction field (SCRF) method.[17] We have used the simple Onsager model with a spherical cavity.[18] The rationale for using a spherical cavity rather than a cavity which follows the molecular shape more faithfully is that we assume that the solute rotates in the solvent and, thus, creates a spherical cavity "on average". This assumption is, of course, a simplification. Furthermore, no specific solvent solute interactions can occur in this model. This specific interaction might be important in some cases.

Table 1. Ionization Potentials, β Values, and STO Type Orbital Exponents ζ for Ruthenium

IP_s	0 eV
IP_p	0 eV
IP_d	−6.98 eV
$\beta_s = \beta_p$	−5.0 eV
β_d	−15.0 eV
ζ_s	1.47
ζ_p	1.47
ζ_d	4.259 (coeff = 0.5342)
	2.0940 (coeff = 0.5927)

Results

INDO Parametrization. Transition metals are not as easy to parametrize as first- and second-row atoms, since the transition metals can adopt several different oxidation states. One way to handle this problem is to search for parameters that reproduce known data from all the different oxidation states. A second way is to assume one oxidation state, e.g., the non-charged atomic state. In the latter case, care has to be taken to also include all close-lying atomic states. In general, transition metals have an s^2d^n atomic configuration, but the s^1d^{n+1} and s^0d^{n+2} states are usually close in energy to the s^2d^n state and will contribute to the measured ionization potentials, which are used as a part of the INDO parametrization. In this work, the first approach has been adopted.

In most of the ruthenium complexes, the ruthenium ion is in the 2+ or 3+ oxidation state. In the vast majority of the complexes in this study, the ruthenium ion is in the 2+ oxidation state, but some complexes with Ru(III) ions are investigated. We have thus used the s^0d^6 ionic state (Ru(II)) to obtain the ionization potentials which are used in the formulas for the Fock matrix elements (see the Appendix). The ruthenium parameters that we propose are collected in Table 1. The parameters are explained in the Appendix.

$[Ru(NH_3)_6]^{2+/3+}$ (I). The INDO/1 method predicts a Ru−N bond distance of 2.091 Å for the Ru(II) complex and 2.078 Å for the Ru(III) complex. All Ru−N bonds and ammine groups are predicted to be almost identical, even though no symmetry is assumed in the calculations on the Ru(II) complex. For the Ru(III) complex, a small distortion of the geometry is obtained. This distortion occurs since the Ru(III) system has one odd electron. The reported bond length is the average bond length. The N−H bond distance is predicted to be 1.057 Å for the Ru(II) complex and 1.060 Å for the Ru(III) complex. The H−N−H bond angle is predicted to be 106.6° and 105.5° for the Ru(II) and Ru(III) complexes, respectively. The experi-

(10) Ford, P.; Rudd, D. F. P.; Gaunder, R.; Taube, H. *J. Am. Chem. Soc*. **1968**, *90*, 1187.
(11) Braddock, J. N.; Meyer, T. J. *J. Am. Chem. Soc.* **1973**, *95*, 3158.
(12) See, for instance: Mackay, K. M.; Mackay, R. A. *Introduction to modern inorganic chemistry*; International Textbook Co.: London, 1981.
(13) GAMESS: Schmidt, M. W.; Baldridge, K. K.; Boatz, J. A.; Elbert, T. S.; Gordon, M. S.; Jensen, J. H.; Koseki, S.; Matsunaga, N.; Nguyen, K. A.; Su, S.; Windus, T. L.; Dupuis, M.; Montgomery J. A., Jr., *J. Comput. Chem.* **1993**, *14*, 1347.
(14) Stevens, W. J.; Basch, H.; Krauss, M. *J. Chem. Phys.* **1984**, *81*, 6026. Stevens, W. J.; Basch, H.; Krauss, M.; Jasien, P. *Can. J. Chem*. **1992**, *70*, 612. Cundari, T. R.; Stevens, W. J. *J. Chem. Phys*. **1993**, *98*, 5555.
(15) STO-3G: Hehre, W. J.; Stewart, R. F.; Pople, J. A. *J. Chem. Phys.* **1969**, *51*, 2657. Hehre, W. J.; Ditchfield, R.; Stewart, R. F.; Pople, J. A. *J. Chem. Phys.* **1970**, *52*, 2769. 6-31G: Ditchfield, R.; Hehre, W. J.; Pople, J. A. *J. Chem. Phys.* **1971**, *54*, 724. Hehre, W. J.; Ditchfield, R.; Pople, J. A. *J. Chem. Phys.* **1972**, *56*, 2257.
(16) ZINDO: Zerner, M. C. Quantum Theory Project, University of Florida, Gainesville, FL.
(17) Karelson, M. M.; Zerner, M. C. *J. Phys. Chem*. **1992**, *96*, 6949.
(18) Onsager, L. *J. Am. Chem. Soc*. **1936**, *58*, 1486.

mental Ru−N bond lengths are 2.144 Å for the Ru(II) complex[8] and 2.104 Å for the Ru(III) complex.[19]

The ab initio geometry optimizations, with the SBK+6-31G basis set, predict a Ru−N bond length of 2.286 Å, which is in surprisingly bad agreement with the experimental findings. With the smaller basis set, SBK+STO-3G, the Ru−N bond distance is predicted to be 2.239 Å, which is in slightly better agreement with the experimental data. Those rather disappointing ab initio results have also been observed in other Hartree−Fock studies of transition metal complex, but then for first-row transition metal complexes.[5] In most of these cases, a much better agreement between experiment and theory is obtained by including electron correlation in the calculation. However, it is believed that correlation effects are of less importance for second-row transition metal complexes (see, for example, ref 4. The importance of basis set and electron correlation on the geometry of $[Ru(NH_3)_6]^{2+}$ has been investigated in greater detail by one of us.[20] When electron correlation is included in the calculation (MP2), the predicted Ru−N bond lengths decrease by 0.04 Å compared to the Hartree−Fock predicted bond lengths, using the same effective core potential (ECP) basis set. With an all-electron basis set, the geometry is predicted in better accord with the observed geometry already at the HF level. At the MP2 level of theory, using an all-electron basis set, the geometry is predicted in good agreement with the observed geometry. Broo[20] suggested that the reason for the rather bad results obtained with the ECP basis set is that the core potential is obtained for the atomic state of the metal. The core potential obtained in this way is not suitable to describe the core electrons in an ionic state of the metal. This is one of the reasons that we use an ionic state of ruthenium for the parametrization since most of the interesting organometallics have the metal in an ionic state.

Meyer used absorption spectroscopy to determine the ligand field splitting of the $[Ru(NH_3)_6]^{2+/3+}$ complexes.[21] The absorption spectrum of the Ru(II) complex has a very weak band at 3.10 eV ($\epsilon = 30$ M^{-1} cm^{-1}) and a somewhat stronger band at 4.51 eV ($\epsilon = 630$ M^{-1} cm^{-1}); both transitions are symmetry forbidden. The INDO/S calculation predicts three transitions at about 3.08 eV and a second band of three transitions at about 4.18 eV. Both bands are due to three $t_{2g}\rightarrow e_g$ ($d\rightarrow d^*$) transitions. The oscillator strengths are predicted to be very small for all the $t_{2g}\rightarrow e_g$ transitions, since the transitions are symmetry forbidden. The observed intensities are due to vibrations, which decrease the symmetry. The calculated absorption spectrum of the Ru(III) complex is more complicated. The INDO/S model predicts 10 transitions with energies between 3.66 and 5.52 eV, all with very small oscillator strengths. Meyer found two bands in the absorption spectrum of the Ru(III) complex located at 3.87 ($\epsilon = 100$ M^{-1} cm^{-1}) and 5.08 eV ($\epsilon = 479$ M^{-1} cm^{-1}).[21]

$[Ru(bpy)_3]^{2+}$ (II). Our second test molecule for the parametrization is $[Ru(bpy)_3]^{2+}$ (**II**). The x-ray crystallographic geometry has been determined by Rillema et al.[9] The INDO/1 predicted geometry is compared with the experimental geometry in Figure 1. The agreement between theory and experiment is remarkably good, except for the outermost part of the bpy ligand, where we predict somewhat longer bond lengths than observed. We believe that this deviation may partially be due to the fact that the accuracy of the experimentally determined geometry decreases with increasing distance from the central metal ion.

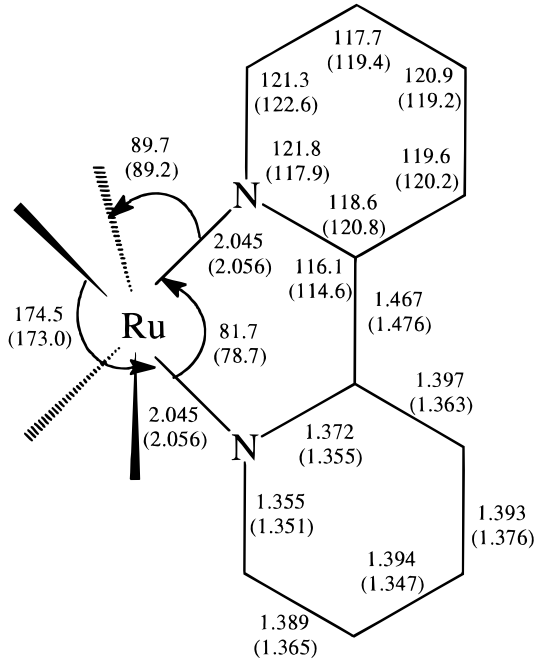

Figure 1. Comparison of the INDO/1 predicted geometry of $[Ru(bpy)_3]^{2+}$ with the x-ray crystallographic determined geometry of $[Ru(bpy)_3][PF_6]_2$.[9]

Table 2. Summary of the Predicted Absorption Spectrum of $[Ru(bpy)_3]^{2+}$, Compared with the Experimental Spectrum Taken in 1.0 M $HClO_4$ Solution[1,23,a]

calcd energy (cm^{-1})	f_{osc}	assignment	exptl energy (cm^{-1})	ϵ_{mol}	assignment
18 000	0.005	$t_{2g}\rightarrow\pi^*$	18 200 sh	∼600	triplet
19 400	0.082	$t_{2g}\rightarrow\pi^*$			
19 400	0.080	$t_{2g}\rightarrow\pi^*$			
19 900	0.160	$t_{2g}\rightarrow\pi^*$	22 000 b	13 800	$t_{2g}\rightarrow\pi^*$
19 900	0.163	$t_{2g}\rightarrow\pi^*$			
27 800	0.066	$t_{2g}\rightarrow\pi^*$			
27 800	0.059	$t_{2g}\rightarrow\pi^*$			
28 000	0.206	$t_{2g}\rightarrow\pi^*$	29 100 sh		$d\rightarrow d^*$
28 000	0.198	$t_{2g}\rightarrow\pi^*$			
28 200	0.123	$t_{2g}\rightarrow\pi^*$			
32 300	0.040	$t_{2g}\rightarrow\pi^*$	31 100 sh		$d\rightarrow d^*$
34 200	0.395	$t_{2g}\rightarrow\pi^* + \pi\rightarrow\pi^*$			
34 300	0.396	$t_{2g}\rightarrow\pi^* + \pi\rightarrow\pi^*$			
35 400	1.326	$t_{2g}\rightarrow\pi^* + \pi\rightarrow\pi^*$	34 900 b	79 000	$\pi\rightarrow\pi^*$
37 800	0.038	$t_{2g}\rightarrow\pi^*$			
37 800	0.038	$t_{2g}\rightarrow\pi^*$			
38 500	0.680	$\pi\rightarrow\pi^* + t_{2g}\rightarrow\pi^*$	39 600 sh	21 800	$t_{2g}\rightarrow\pi^*$
40 900	0.050	$\pi\rightarrow\pi^*$			
40 900	0.050	$\pi\rightarrow\pi^*$			
41 600	0.285	$\pi\rightarrow\pi^*$	41 100 s	25 000	$t_{2g}\rightarrow\pi^*$

[a] Abbreviations used: sh, shoulder; s, sharp, b, band; t_{2g}, metal-centered MO with t_{2g}-like symmetry; π and π^* denote ligand MOs with mostly π character.

The absorption spectrum of **II** as predicted by the INDO/S model is summarized in Table 2. The first transition at about 18 000 cm^{-1} may be identified with the shoulder in the low-energy tail of the observed absorption spectrum, which has been assigned to a triplet state due to the long lifetime of the first excited state.[1] However, we predict the lowest triplet state at 13 900 cm^{-1}. The shoulders at 29 100 and 31 100 cm^{-1} were suggested to be due to metal $d\rightarrow d^*$ transitions,[1] but we calculate several $M\rightarrow L$ transitions and no $d\rightarrow d^*$ transitions at all in that region of the spectrum.

$[Ru(NH_3)_5\text{-}pyz]^{2+}$ (III). The X-ray crystallographic geometry of $[Ru(NH_3)_5pyz](BF_4)_2$ has been determined by Gress et al.[24] In the crystal, the Ru−N_{pyz} bond is significantly shorter

(19) Peresie, H. J.; Stanko, J. A. *Chem. Commun.* **1970**, 1674.
(20) Broo, A. *Int. J. Quantum. Chem., Quantum Chem. Symp.* **1996**, *30*, 119.
(21) Meyer, T. Ph.D. Dissertation, Stanford University, Stanford, CA, 1966; p 30.

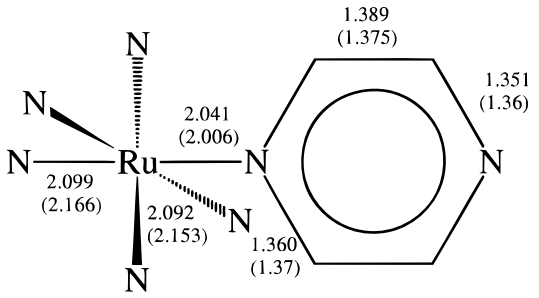

Figure 2. Comparison of the geometry of $[Ru(NH_3)_5pyz]^{2+}$, as predicted by the INDO/1 model Hamiltonian, with the X-ray determined geometry of $[Ru(NH_3)_5pyz][BF_2]$.[24]

than the ruthenium−ammine bonds, and the ruthenium−*trans*-ammine bond is even somewhat longer than the other four Ru−NH_3 bonds. The predicted geometry is compared with the X-ray geometry in Figure 2. The calculated geometry has the same Ru−N bond length relation as the experimental geometry; however, the backbonding contribution to the Ru−N_{pyz} bond seems to be smaller in the calculated geometry than observed.

Using the theoretical geometry, we have calculated the absorption spectrum of $[Ru(NH3)_5pyz]^{2+}$ in a vacuum. The experimental spectrum is taken in dimethylformamide solution.[10] Two bands occur in the UV/vis spectrum: the first and most intense band is located at about 21 200 cm^{-1} (ϵ = 10 700 M^{-1} cm^{-1}), and the second band is found at about 39 000 cm^{-1}. Furthermore, the position of the first peak is sensitive to the solvent and is shifted to the lower energies with increasing polarity of the solvent.[10] The gas phase calculation predicts a metal-to-ligand charge transfer (MLCT) transition at 28 600 cm^{-1} (f_{osc} = 0.35) and a second band at 41 800 cm^{-1} (f_{osc} = 0.29). The second band has predominantly $\pi \rightarrow \pi^*$ character and a small contribution from a MLCT transition. In order to estimate the solvent effect on the absorption spectrum, a SCRF calculation was performed. Indeed, the MLCT band is calculated at much lower energy in DMF solution than in vacuum. The first band is now located at 25 900 cm^{-1} (f_{osc} = 0.60), which still is 5700 cm^{-1} too high, and the second band is found at 39 100 cm^{-1} (f_{osc} = 0.26). A similar solvent shift was calculated by Broo and Larsson using a similar SCRF model and the CNDO/S model Hamiltonian.[4a] Unfortunately, in the work by Broo and Larsson, the calculated solvent shift for **III** was compared with the experimental solvent shift for **IV**.

$[Ru(NH_3)_5py]^{2+}$ (IV). To the best of our knowledge, no experimental geometry has been published for complex **IV**. The predicted geometry is very similar to the geometry of **III**. The Ru−N_{py} bond length is 2.037 Å, the Ru−NH_3 bonds are 2.091 Å, and the Ru−NH_3(trans) is 2.094 Å.

Ford et al. have investigated the spectroscopy of **IV** in a number of polar solvents.[10] Several attempts have been made to simulate the red shift of the absorption spectrum due to solvent interactions.[2d,e,4a] Stavrev et al. reported INDO/S calculations with a different set of parameters for ruthenium than those used in this work, where they suggest that part of the solvent shift is due to charge transfer from the solvent to the solute.[2e] They simulated the solvation process by including several water molecules in the calculation. In vacuum we predict two strong bands: at 30 100 cm^{-1} (f_{osc} = 0.34) we find the MLCT band, and at 43 100 cm^{-1} (f_{osc} = 0.28) the $\pi \rightarrow \pi^*$ is located. Using the SCRF model to include nonspecific solvent effects in the calculation, we predict the MLCT band, in water, at 26 300 cm^{-1} (f_{osc} = 0.41) and the $\pi \rightarrow \pi^*$ at 41 500 cm^{-1} (f_{osc} = 0.21). In the experimental spectrum, recorded in water solution, the charge transfer band is found at 24 600 cm^{-1} (ϵ = 7800 M^{-1} cm^{-1}), and the $\pi \rightarrow \pi^*$ band is located at 41 000 cm^{-1} (ϵ = 4600 M^{-1} cm^{-1}). Our "gas phase" transition energies and oscillator strengths differ very much from the values that were predicted by Stavrev et al.[2e] and by Zeng et al.[2d] The large differences are due to the differences in the Ru parameters used in this work and the Ru parameters used in the two other works. Furthermore, when the "standard INDO" Ru parameters are used, the d_π (d_{xz} in our coordinate system) interactions with the pyridine π and π^* orbitals are small. For most of the previously reported complexes in this work, the MLCT transition has been calculated at 2000 cm^{-1} too low energy. For **IV**, we predict the MLCT band too high in energy by about the same amount. We believe that specific solvent−solute interactions are needed to sufficiently account for all the solvent shift observed for **IV**, as was suggested and modeled by Stavrev et al.[2e]

Table 3. Important Bond Lengths of the Creutz−Taube Ion (**V**) As Predicted by the INDO/1 Model, Compared with the Experimental Bond Lengths Presented by Fürholz et al.[25]

	$V \cdot Cl_5$	$V \cdot (tos)_5$	INDO/1
Ru(1)−N_{pyz}	2.002	1.971	2.056
Ru(2)−N_{pyz}	2.002	1.995	2.067
Ru(1)−NH_3(trans)	2.135	2.134	2.079
Ru(2)−NH_3(trans)		2.119	2.094
Ru(1)−NH_3(cis)	2.110	2.112	2.085
Ru(2)−NH_3(cis)		2.114	2.096

$[Ru(NH_3)_5$-pyz-$Ru(NH_3)_5]^{4+/5+}$ (V). The question of whether the odd electron in the 5+ complex **V** is localized or delocalized has been debated for a long time (see, for instance, ref 4a and references in there). Now, both experimental[25] and theoretical[3d,4a] investigations support the delocalized picture. In the work by Zhang et al., no geometry optimization was performed; however, different geometries were used to investigate whether a localized or a delocalized description of V^{5+} is suitable.[3d] Here, for the first time, we present a full geometry optimization of the so-called Creutz−Taube ion. In Table 3, the theoretical Ru−N bond lengths are compared with the corresponding experimental bond lengths reported by Fürholz et al.[25] The *p*-toluenesulfonate salt of the Creutz−Taube ion has two different ruthenium sites, while the chloride salt has indistinguishable sites. The INDO/1 model predicts a somewhat nonsymmetric geometry; as a consequence, a small localization of the Ru d electrons occurs. The total Mulliken charges of the two ruthenium sites differ by 0.2 electron. Our result indicates that the ground state of the Creutz−Taube ion is unsymmetric, in contrast to what was found by Zhang et al.[3d] Zhang et al. performed Hartree−Fock−Slater calculations on a symmetric and an asymmetric geometry of the Creutz−Taube ion. They did not observe any charge localization when using the asymmetric geometry. The asymmetric geometry was constructed from the crystallographic geometry of the 4+ and 6+ complexes of **V**, which is much more asymmetric than the INDO/1 predicted geometry presented in this work.

The absorption spectra of $V^{4+/5+/6+}$ were first reported by Creutz and Taube.[26] They reported that the absorption spectrum of V^{5+} was rather different from those of V^{4+} and V^{6+}. At very low energy (6400 cm^{-1}, ϵ = 5500 M^{-1} cm^{-1}), a rather intense band appears that is not observed for the other two

(22) Durham, B.; Wilson, S. R.; Hodgson, D. J.; Meyer, T. J. *J. Am. Chem. Soc.* **1980**, *102*, 600.
(23) Baddock, J. N.; Meyer, T. J. *J. Am. Chem. Soc.* **1973**, *95*, 3158.
(24) Gress, M. E.; Creutz, C.; Quicksall, C. O. *Inorg. Chem.* **1981**, *20*, 1522.
(25) Fürholz, U.; Bürgi, H.-B.; Wagner, F. E.; Stebler, A.; Ammeter, J. H.; Krausz, E.; Clark, R. J. H.; Stead, M. J.; Ludi, A. *J. Am. Chem. Soc.* **1984**, *106*, 121.
(26) Creutz, C.; Taube, H. *J. Am. Chem. Soc.* **1969**, *91*, 3988.

Table 4. Predicted Absorption Spectrum of $[Ru(NH_3)_5$-pyz-$Ru(NH_3)_5]^{5+}$, Compared with the Observed Spectrum[a]

this work E (cm^{-1})	f_{osc} and assignment	CASSCF E (cm^{-1})	HFS-DVM E (cm^{-1})	exptl E (cm^{-1})
5900	sf $t_{2g}\rightarrow$N		2260 $t_{2g}\rightarrow$N	2000 MCD
6000				
6200	sf $t_{2g}\rightarrow$N		2900 $t_{2g}\rightarrow$N	4000 MCD
6200				
4900	0.007 B→N	3 000	6600 IT(B→N)	6400 IT
9600				12 000 sh
16 300−18 200	8 transitions, sf $t_{2g}\rightarrow$N			12 800 MCD
20 500	0.003 N→A + $t_{2g}\rightarrow\pi^*$			17 400 MCD
21 100	0.538 N→A	19 700	19 000 N→A	17 700 $t_{2g}\rightarrow\pi^*$
			21 200 $t_{2g}\rightarrow$A	20 400 MCD
33 900	0.071 mixed		33 500 $t_{2g}\rightarrow e_g$	37 000 sh
39 300	0.126 $\pi\rightarrow\pi^*$		37 700 B→e_g	
			40 400 $\pi\rightarrow$A	
39 400	0.077 $t_{2g}\rightarrow\pi^*$		42 800 $\pi\rightarrow\pi^*$	39 700 $\pi\rightarrow\pi^*$
	$\pi\rightarrow\pi^*$			

[a] B, A, and N denote a bonding, an antibonding, and a nonbonding combination of Ru(1) $4d_{xz}$, π, and Ru(2) $4d_{xz}$. Mixed means mixed character, large contributions of double excited determinants; sf denotes spin-forbidden transition.

complexes. That band was ascribed to a Ru(II)-to-Ru(III) intervalence transition, which indicates that the odd electron should be localized on one of the metal sites. Later, this band was described as a transition from a MO that has both metal and pyrazine π character to an MO that has the same type of character, thus, a complete delocalized picture. Furthermore, the band position is solvent independent, which also indicates a delocalized picture.[25,26] Broo and Larsson calculated the transition energies for the two first allowed transitions for $\mathbf{V}^{5+}$, using a complete active space self-consistent field (CASSCF) model with a minimal basis set.[4a] They found that the second band was described by a rather complicated mixture of single and double excited determinants. Furthermore, a method that only includes single excited determinants (CIS) will not be suitable to model the spectrum of $\mathbf{V}^{5+}$. We have performed a INDO/S calculation followed by a configuration interaction that includes all single and double excitations (CISD) in an active space containing all occupied metal MOs, the pyrazine π orbitals, and the three unoccupied pyrazine π^* orbitals. The predicted absorption spectrum is reported in Table 4. The relative importance of the double excited determinants for the description of the second strong band was confirmed by a CIS calculation of the absorption spectrum, which gives a rather different spectrum. The crystallographic geometry was used for the spectrum calculation for comparison reasons, but if the INDO/1 geometry is used, the predicted spectrum is almost unchanged, even though some localization of the MOs before the CI is observed. Thus, the CI treatment restores the delocalized picture. We conclude that the reported spectrum agrees well with the observed spectrum in almost all details, in contrast to previous theoretical work. However, the intensity (oscillator strength) of the "intervalence" charge transfer transition is calculated much too low compared to the second strong metal-to-π^* transition. We believe that vibration borrowing could account for the "missing" intensity.

The absorption spectrum of $\mathbf{V}^{4+}$ is, perhaps, less interesting since no spectacular absorptions are reported for this complex. However, we reproduce the observed spectrum with good accuracy. Creutz and Taube[26] reported two bands for $\mathbf{V}^{4+}$, a MLCT band at about 18 300 cm^{-1} (ϵ = 30 000 M^{-1} cm^{-1}) and band at 38 500 cm^{-1} ($\pi\rightarrow\pi^*$) with about one-third of the intensity of the MLCT band. A shoulder at about 37 000 cm^{-1} is also observed. We predict a MLCT peak at 20 200 cm^{-1} (f_{osc} = 1.068) and a second MLCT peak at 24 400 cm^{-1} (f_{osc} = 0.014). The second MLCT peak might be responsible for the small asymmetry of the observed intense MLCT band. At 37 700 (f_{osc} = 0.018) and 38 700 (f_{osc} = 0.269), we predict two $\pi\rightarrow\pi^*$ peaks.

Table 5. Predicted Absorption Spectrum of One Conformer of $[Ru(py)_6]^{2+}$, Compared with the Observed Spectrum Taken in Acetonitrile[27]

this work E (cm^{-1})	f_{osc}	assignment	obsd band maximum E (cm^{-1})	ϵ_{mol} (M^{-1} cm^{-1})
16 900	0.051	$t_{2g}\rightarrow\pi^*$		
17 800	0.089	$t_{2g}\rightarrow\pi^*$		
22 900	0.121	$t_{2g}\rightarrow\pi^*$		
23 100	0.250	$t_{2g}\rightarrow\pi^*$		
24 400	0.359	$t_{2g}\rightarrow\pi^*$	29 300	22 800 $t_{2g}\rightarrow\pi^*$
29 300	0.014	$t_{2g}\rightarrow\pi^*$		
29 800	0.057	$t_{2g}\rightarrow\pi^*$		
31 000	0.489	$t_{2g}\rightarrow\pi^* + \pi\rightarrow\pi^*$		
32 300	0.001	$t_{2g}\rightarrow\pi^*$		
34 500	0.512	$t_{2g}\rightarrow\pi^* + \pi\rightarrow\pi^*$		
35 200	0.060	$t_{2g}\rightarrow\pi^*$		
37 300	0.891	$\pi\rightarrow\pi^*$	36 800	5700
38 400	0.008	$t_{2g}\rightarrow\pi^*$		
38 600	0.066	$\pi\rightarrow\pi^*$		
39 700	0.043	$\pi\rightarrow\pi^*$		
41 500	0.075	$\pi\rightarrow\pi^*$		
42 500	1.004	$\pi\rightarrow\pi^*$	41 200	22 800 $\pi\rightarrow\pi^*$

$[Ru(py)_6]^{2+}$ (VI). A geometry optimization of **VI** is very complicated, since there are several possible conformers due to the free rotation of the pyridine ligands. We have optimized one geometry assuming four of the pyridines to be oriented along *y* and *z* axes, and the remaining two pyridines' planes form a 45° angle with the *z* and *y* axes. The trans pyridines were placed in a coplanar conformation. The final geometry has two different Ru−N bond lengths, 2.070 (four) and 2.039 Å (two). In an X-ray crystallographic study of $[Ru(py)_6][BF_4]_2$, Templeton determined the Ru−N bond lengths to be between 2.10 and 2.14 Å, with an average bond length of 2.118 Å.[27] Moreover, the trans pyridine was oriented in such a way that the ring planes formed angles of 90.7°, 65.5°, and 29.9°. We have not tried to obtain the global energy minimum, but rather kept a high symmetry. It is very likely that there are several local energy minima close in energy and geometry. Thus, the reported geometry represents one possible geometry out of several possible conformers.

The predicted absorption spectrum is summarized in Table 5. Unfortunately, only band maxima rather than the full observed spectrum were reported by Templeton.[27] That makes

(27) Templeton, J. L. *J. Am. Chem. Soc.* **1979**, *101*, 4906.

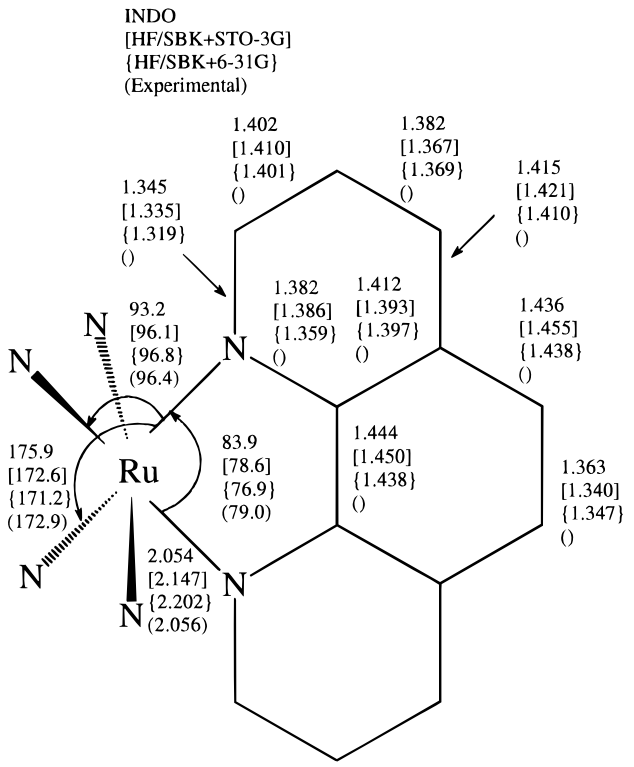

Figure 3. Comparison of the geometry of $[Ru(phen)_3]^{2+}$ predicted by the INDO/1 model Hamiltonian and ab initio Hartree−Fock calculations, using two different basis sets.

a comparison between that calculated and observed spectra troublesome. The observed band at 29 300 cm^{-1} may originate from several metal-to-ligand transitions that are calculated to lie between 16 000 and 31 000 cm^{-1}. Several of the predicted transitions are close in energy, and the weak peaks (small oscillator strength) would not be possible to resolve due to more intense overlapping bands. Solvent motions and internal motions, due to the rather free rotation of the pyridine ligands, will make the MLCT band very broad. The calculated spectrum suggests that the observed MLCT band should have some structure, with two maxima at about 25 000 and 31 000 cm^{-1} and a long tail to the low-energy side. The observed band at 36 800 cm^{-1} was not assigned in the work by Templeton.[27] We suggest that the calculated transitions at 34 500 ($\pi\rightarrow\pi^*$ and MLCT) and at 37 300 cm^{-1} ($\pi\rightarrow\pi^*$) may be identified as the observed band at 36 800 cm^{-1}, giving the band a mixed character. The agreement between the predicted and observed spectrum is good at the high-energy side, but the low-energy part is reproduced rather poorly. A better resolved absorption spectrum is needed for a more reliable comparison.

$[Ru(phen)_3]^{2+}$ and $[Ru(phen)_2dppz]^{2+}$ (VII and VIII). The geometry of **VII** has been optimized with the INDO/1 model and with ab initio calculations using two different basis sets. The predicted geometries are reported in Figure 3. The ab initio calculations predict much longer Ru−N bond lengths than does the INDO/1 model, which was also the case for the $[Ru(NH_3)_6]^{2+}$ complex. No high-quality x-ray crystallographic data are available for **VII**, but preliminary work[32] indicates that the INDO/1 predicted Ru−N bond lengths are in better agreement with crystallographic data than the ab initio predicted Ru−N bond lengths are. All three models predict similar ligand geometries. The largest differences are found close to the metal ion. The INDO/1 geometry of **VIII** is reported in Figure 4.

The predicted absorption spectrum of **VII,** together with the spectrum of **VIII,** is summarized in Table 6. A more detailed discussion about these spectra has already been published.[28]

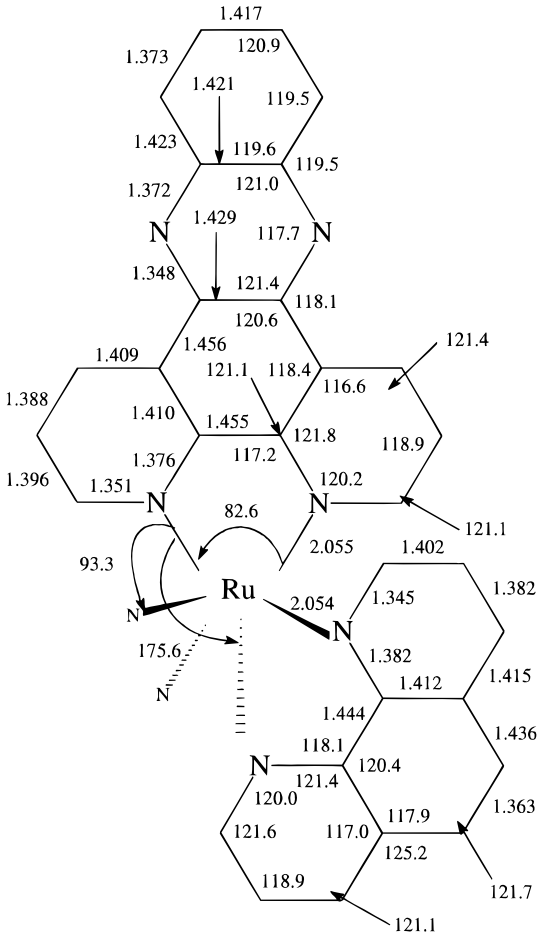

Figure 4. INDO/1 predicted geometry of $[Ru(phen)_2dppz]^{2+}$.

$[Ru(bpy)_2(py)_2]^{2+}$ (trans) (IX). Two different Ru−N bond lengths are obtained in the geometry optimization, $Ru-N_{bpy} = 2.100$ Å and $Ru-N_{py} = 2.040$ Å. The π backbonding effect is larger for the pyridine ligands since they are not as sterically restrained as the bpy ligands are to interact with the metal.

The predicted absorption spectrum of **IX** is reported in Table 7. Some new assignments of the first observed peaks are proposed. Especially notable is the shoulder at about 23 900 cm^{-1}, which has previously been assigned to a $t_{2g}\rightarrow\pi^*_{bpy}$ charge transfer transition,[29] while we find a $t_{2g}\rightarrow\pi^*_{py}$ transition with large oscillator strength at 24 100 cm^{-1}. Experimentally, no $t_{2g}\rightarrow\pi^*_{py}$ transition has been assigned in that energy region.

$[Ru(phen)_2biquin]^{2+}$ (X). The predicted geometry of **X** is reported in Figure 5. Metal binding reduces the local symmetry of the biquin due to induced ring strain and steric effects. All three ligands are predicted to be somewhat nonplanar. The biquin ligand is twisted 6.7° around the central C−C bond, and the phenyl ring planes are forming an angle of about 4.5° with the pyridine planes. The complex has almost C_2 symmetry, but the total symmetry is C_1. The symmetry lowering affects the absorption spectrum since more transitions will be allowed due to the reduced symmetry as opposed to, for example, the $Ru(bpy)_3$ and the $Ru(phen)_3$ complexes that have D_3 symmetry. The predicted absorption spectrum of **X** is compared to the observed spectrum in Table 8.[30]

$[Ru(H_2O)_6]^{2+/3+}$ and $[Ru(bpy)_2(OH)(H_2O)]^{2+}$ (XI and XII). As a consistency test for the proposed ruthenium parameters,

(28) Lincoln, P.; Broo, A.; Nordén, B. *J. Am. Chem. Soc.* **1996**, *118*, 2644.
(29) Bryant, G. M.; Fergusson, J. E.; Powell, H. K. J. *Aust. J. Chem.* **1971**, *24*, 257.
(30) Klassen, D. M. *Chem. Phys. Lett.* **1982**, *93*, 383.

Table 6. INDO/S Predicted Absorption Spectra of $[Ru(phen)_3]^{2+}$ and $[Ru(phen)_2dppz]^{2+}$ [a]

$[Ru(phen)_3]^{2+}$				$[Ru(phen)_2dppz]^{2+}$				
calcd		exptl[11]		calcd			exptl[33a]	
E ($\times 10^3$ cm^{-1})	f_{osc} D_3	E ($\times 10^3$ cm^{-1})	$\epsilon/10^3$	E ($\times 10^3$ cm^{-1})	f_{osc} C_2	assignment	E ($\times 10^3$ cm^{-1})	$\epsilon/10^3$
19.7	0.08 E			19.6	0.17 A	$t_{2g}\rightarrow\pi^*$	21.6	
19.7	0.09 E	22.3	18.4	19.7	0.12 B	$t_{2g}\rightarrow\pi^*$	22.3	
20.1	0.12 E			20.0	0.17 A	$t_{2g}\rightarrow\pi^*$	23.3	20.0
20.1	0.12 E			20.2	0.09 B	$t_{2g}\rightarrow\pi_*$		
24.3	0.24 E			24.2	0.21 B	$t_{2g}\rightarrow\pi_{phen}$		
24.3	0.27 E	23.7	17.6	24.3	0.05 B	$t_{2g}\rightarrow\pi_{phen}$	23.8	
24.8	0.16 A_2			24.6	0.10 B	$t_{2g}\rightarrow\pi_{phen}$		
				25.5	0.25 A	$t_{2g}\rightarrow\pi_{dppz}$	26.6	
				27.0	0.22 A	$\pi\rightarrow\pi^*_{dppz}$	27.0	21.8
				27.4	0.13 B	$\pi\rightarrow\pi^*_{dppz}$		
				33.2	0.23 B	$\pi\rightarrow\pi^*_{dppz}$		
				33.6	1.17 A	$\pi\rightarrow\pi^*_{dppz}$	35.5	
				33.6	0.11 A	$\pi\rightarrow\pi^*_{dppz}$		
				36.6	0.06 B	mixed		
				36.6	0.29 A	$\pi\rightarrow\pi^*_{dppz}$		
37.0	0.45 E			37.1	0.16 A	$\pi\rightarrow\pi^*_{dppz}$	37.1	
37.0	0.45 E	38.2	112	37.2	0.14 A	$t_{2g}\rightarrow\pi_{phen}$		
38.7	1.86 A_2			37.3	0.30 B	$t_{2g}\rightarrow\pi_{phen}$		
				37.8	0.09 B	$\pi\rightarrow\pi^*_{dppz}$		
				38.2	0.05 A	$\pi\rightarrow\pi^*_{dppz}$		
				38.8	1.42 B	$\pi\rightarrow\pi^*_{phen}$	37.7	117

[a] The D_3 symmetry labels have been used to classify the transition of the $[Ru(phen)_3]^{2+}$ complex, and the C_2 symmetry labels have been used for the $[Ru(phen)_2dppz]^{2+}$ complex.

Table 7. Comparison of INDO/S Predicted Absorption Spectrum of *trans*-$[Ru(bpy)_2(py)_2]^{2+}$ with Observed Absorption Spectrum of $[Ru(bpy)_2(py)_2]$ Taken in Methanol Solution[29]

INDO/S			obsd		
E (cm^{-1})	f_{osc}	assignment	E (cm^{-1})	ϵ (M^{-1} cm^{-1})	assignment
17 800	0.287	$t_{2g}\rightarrow\pi_{bpy}$	21 740	7840	$t_{2g}\rightarrow\pi_{bpy}$
24 100	0.637	$t_{2g}\rightarrow\pi_{py}$	23 920	4520	sh
26 300	0.072	$t_{2g}\rightarrow\pi_{bpy}$			
27 600	0.349	$t_{2g}\rightarrow\pi_{bpy}$	29 870	11 100	$t_{2g}\rightarrow\pi_{bpy}$
30 300	0.028	$t_{2g}\rightarrow\pi_{bpy} + \pi\rightarrow\pi^*_{bpy}$			
34 400	1.211	$\pi\rightarrow\pi^*_{bpy} + t_{2g}\rightarrow\pi_{bpy}$	34 530	50 200	$\pi\rightarrow\pi^*_{bpy}$
36 800	0.334	$t_{2g}\rightarrow\pi_{bpy} + \pi\rightarrow\pi^*_{bpy}$	36 100	17 500	sh
41 100	0.368	$t_{2g}\rightarrow\pi_{bpy}$	39 370		sh
		$\pi\rightarrow\pi^*_{bpy}$			
42 200	0.674	$\pi\rightarrow\pi^*_{py} + t_{2g}\rightarrow\pi_{py}$	40 980	23 850	$\pi\rightarrow\pi^*_{bpy}$
42 400	0.331	$\pi\rightarrow\pi^*_{bpy}$			

we have also optimize the geometry of $[Ru(H_2O)_6]^{2+/3+}$ and $[Ru(bpy)_2(OH)(H_2O)]^{2+}$. For $[Ru(H_2O)_6]^{2+}$, we obtain an average Ru−O bond distance of 2.013 Å, compared to the observed 2.122 Å.[31] The predicted geometry is close to D_{2h} symmetry, and if the D_{2h} symmetry is enforced, the geometrical parameters are not altered significantly. The predicted Ru−O bond lengths are too short by more than 0.1 Å compared with the experimental data. The Ru(III)−O bond lengths are predicted to be 2.008, 1.967, and 1.965 Å (average is 1.980 Å), compared to an average Ru(III)−O bond length of 2.029 Å. Thus, we predict a bond length change by only 0.033 Å compared to the observed 0.093 Å when the oxidation state is changed. For $[Ru(bpy)_2(OH)(H_2O)]^{2+}$, we have assumed a singlet ground state. Other spin states are possible since the ruthenium has formally an oxidation state of 3+, but most Ru(III) complexes are low-spin complexes. The crystallographic geometry is somewhat distorted, and the bpy ligands are twisted, so that the pyridine planes form an angle of 10°.[22] Only the average metal−ligand bond lengths are reported. The calculation gives naturally two Ru−O distances due to the differences in the ligands. The Ru−OH_2 bond length is predicted to 2.042 Å, and the Ru−OH bond length is 1.925 Å; the average Ru−O bond length is thus 1.984 Å, which should be compared with the observed average bond length of 2.007 Å. The Ru−N bond lengths are calculated to be 2.098 and 2.094 Å, which also are in good agreement with the observed 2.090 and 2.099 Å.[22] The bpy ligands are calculated to be planar. The deviation between the theoretical and observed geometry of the bpy ligands is likely due to crystal packing forces.

Modeling DNA Binding of $[Ru(phen)_2dppz]^{2+}$. It has been shown that the $[Ru(phen)_2dppz]^{2+}$ and the $[Ru(bpy)_2dppz]^{2+}$ complexes bind with DNA in an intercalating mode.[28,33,34] There has been an ongoing debate over from which groove the intercalation occurs. Barton and co-workers have suggets that the binding occurs from the major grove.[34] However, we believe that there are firm evidences for the minor grove intercalation of the DNA helix.[28,34] To estimate the geometry of the $[Ru(phen)_2dppz]^{2+}$−DNA complex, a partial geometry optimization of the complex was done using the molecular

(31) Bernhard, P.; Bürgi, H.-B.; Hauser, J.; Lehmann, H.; Ludi, A. *Inorg. Chem.* **1982**, *21*, 3936.

(32) Personal comunication with Göran Svensson, Inorganic Chemistry, CTH, Göteborg.

(33) (a) Hjort, C.; Lincoln, P.; Nordén, B. *J. Am. Chem. Soc.* **1993**, *115*, 3448. (b) Haq, I.; Lincoln, P.; Suh, D.; Nordén, B.; Chowhry, B. Z.; Chaires, J. B. *J. Am. Chem. Soc.* **1995**, *117*, 4788. (c) Tuite, E.; Lincoln, P.; Nordén, B. *J. Am. Chem. Soc.* **1997**, *119*, 239.

(34) Freidman, A. E.; Kumar, C. V.; Turro, N. J.; Barton, J. K. *Nucleic Acids Res.* **1991**, *19*, 2595. Hartshorn, R. M.; Barton, J. K. *J. Am. Chem. Soc.* **1992**, *114*, 5919. Turro, C.; Bossmann, S. H.; Jenkins, Y.; Barton, J. K.; Turro, N. J. *J. Am. Chem. Soc.* **1995**, *117*, 9026.

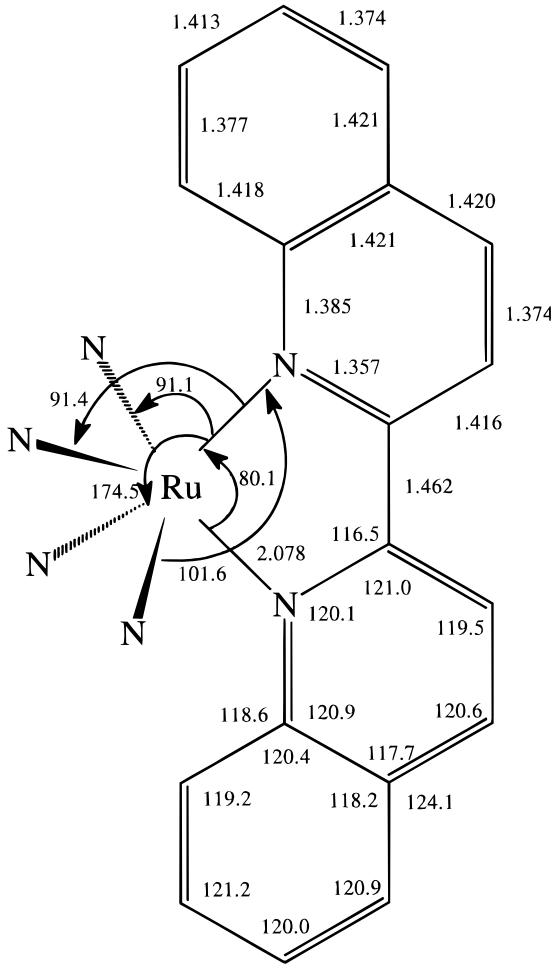

Figure 5. INDO/1 predicted geometry of $[Ru(bpy)_2biquin]^{2+}$.

Table 8. Comparison of INDO/S Predicted Absorption Spectrum with Observed Absorption Spectrum of $[Ru(phen)_2biquin]^{2+}$ [30]

INDO/S			obsd spectrum and assignments	
E (cm^{-1})	f_{osc}	assignment	E (cm^{-1})	ϵ (M^{-1} cm^{-1})
18 900	0.235	$t_{2g}\rightarrow\pi^*_{biquin}$	19 100	9480 $t_{2g}\rightarrow\pi^*_{biquin}$
19 200	0.051	$t_{2g}\rightarrow\pi^*$		
21 000	0.103	$t_{2g}\rightarrow\pi^*_{phen}$	22 800	9630 $t_{2g}\rightarrow\pi^*_{phen}$
23 900	0.153	$t_{2g}\rightarrow\pi^*$	26 500	22 500
25 100	0.085	$t_{2g}\rightarrow\pi^*$		
25 500	0.050	$t_{2g}\rightarrow\pi^*$		
27 300	0.168	$t_{2g}\rightarrow\pi^*$	27 900	19 800
29 300	0.910	$\pi\rightarrow\pi^* + t_{2g}\rightarrow\pi^*$	29 800	21 900
33 800	0.304	$t_{2g}\rightarrow\pi^*$	32 700	20 900
33 900	0.161	$t_{2g}\rightarrow\pi^*$		
35 600	0.063	$\pi\rightarrow\pi^* + t_{2g}\rightarrow\pi^*$		
36 800	0.518	$\pi\rightarrow\pi^*$		
37 400	0.081	$\pi\rightarrow\pi^*$		
37 500	0.221	$\pi\rightarrow\pi^*$		
37 700	0.515	$\pi\rightarrow\pi^* + t_{2g}\rightarrow\pi^*$		
38 300	0.121	$\pi\rightarrow\pi^*$		
38 600	0.963	$\pi\rightarrow\pi^*$	37 700	97 400 $\pi\rightarrow\pi^*$
38 900	0.181	$\pi\rightarrow\pi^*$		
39 200	0.137	$\pi\rightarrow\pi^*$		
39 200	0.137	$\pi\rightarrow\pi^*$		
40 800	0.602	$\pi\rightarrow\pi^*$		
41 200	0.152	$\pi\rightarrow\pi^*$		
41 700	0.219	$\pi\rightarrow\pi^*$		

mechanics (MM) module in the HyperChem 4.5 molecular modeling program package.[35] The AMBER force field was used for the DNA part of the complex. The geometry of the $[Ru(phen)_2dppz]^{2+}$ complex was kept as predicted by the INDO method geometry, and the 12-mer of poly(dA-dT) was allowed to fully relax in the geometry optimization. An atomic charge of +1.2 was assigned to the ruthenium ion, and an atomic charge of −0.2 was assigned to each nitrogen atom bonded to the metal ion. All other atoms of the $[Ru(phen)_2dppz]^{2+}$ complex were given a zero atomic charge. These charges correspond approximately to the Mulliken charges from INDO calculation of the $[Ru(phen)_2dppz]^{2+}$ complex. The AMBER iron van der Waals parameters was used for ruthenium. Since the $[Ru(phen)_2dppz]^{2+}$ complex was not allowed to move in the MM calculation, no extra parameters were required.

(35) HyperChem Release 4.5, Hypercube Inc. 1995.

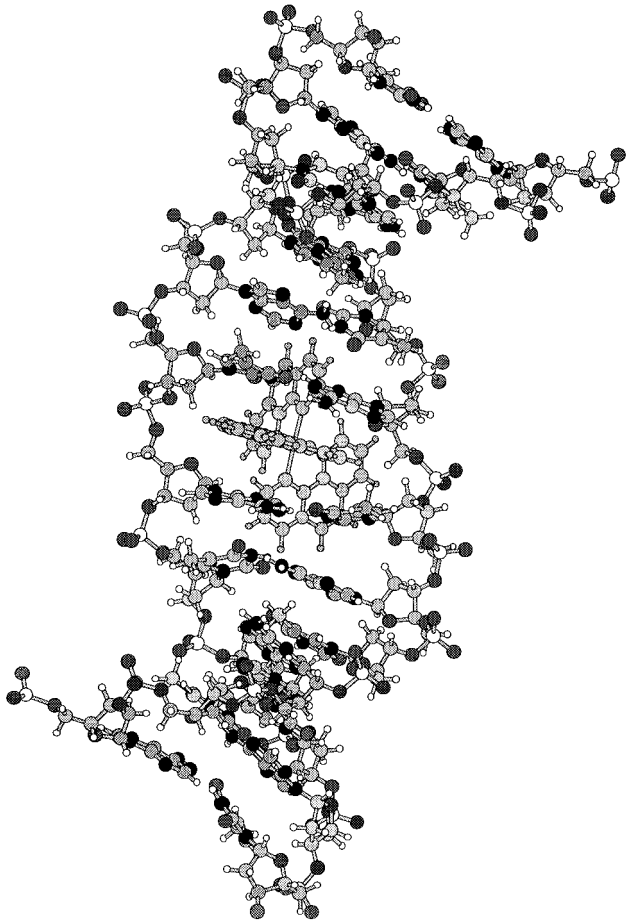

Figure 6. Molecular mechanics predicted geometry of the 12-mer poly(dA-dT) double helix with a $[Ru(phen)_2dppz]^{2+}$ complex intercalated in the minor grove.

The final geometry of the $[Ru(phen)_2dppz]^{2+}$−poly(dA-dT) is depicted in Figure 6. The DNA double helix has been partly unwound by the insertion of the metal complex. A pocket has been formed, and two base pairs up and down from the pocket have been heavily distorted. The ends of the poly(dA-dT) double helix are also partly unwound. The present study represents just a rough description of $[Ru(phen)_2dppz]^{2+}$−DNA intercalating.

The two base pairs closest to the $[Ru(phen)_2dppz]^{2+}$ complex were extracted from the MM minimized geometry. The effect of DNA binding on the calculated absorption spectrum of the $[Ru(phen)_2dppz]^{2+}$ complex was then calculated using the INDO/S method. The base pairs were represented by point charges located at the MM predicted positions for these atoms. The magnitude of the charges was taken as the atomic charges from the AMBER force field. The first band of the absorption spectrum of $[Ru(phen)_2dppz]^{2+}$ was found to be slightly red shifted, with respect to the free solution spectrum, upon DNA binding.[28] The band form of the two first bands are also

Table 9. Comparison between the Predicted Spectrum of Free $[Ru(phen)_2dppz]^{2+}$ and DNA Bonded $[Ru(phen)_2dppz]^{2+}$

$Ru(phen)_{2dppz}]^{2+}$			$[Ru(phen)_{2dppz}]^{2+}$ bonded to DNA		
E ($\times 10^3$ cm^{-1})	f_{osc}	assignment	E ($\times 10^3$ cm^{-1})	f_{osc}	assignment
19.6	0.17	$t_{2g}\rightarrow\pi^*$	18.8	0.18	$t_{2g}\rightarrow\pi^*_{phen}$
19.7	0.12	$t_{2g}\rightarrow\pi^*$	20.1	0.12	$t_{2g}\rightarrow\pi^*_{phen}$
20.0	0.17	$t_{2g}\rightarrow\pi^*$	22.3	0.25	$t_{2g}\rightarrow\pi^*$
20.2	0.09	$t_{2g}\rightarrow\pi^*$	22.9	0.26	$t_{2g}\rightarrow\pi^*_{phen}$
24.2	0.21	$t_{2g}\rightarrow\pi_{phen}$	23.5	0.09	$t_{2g}\rightarrow\pi^*_{phen}$
24.3	0.05	$t_{2g}\rightarrow\pi_{phen}$	26.5	0.07	$t_{2g}\rightarrow\pi^*$
24.6	0.10	$t_{2g}\rightarrow\pi_{phen}$	28.1	0.12	$t_{2g}\rightarrow\pi^*_{dppz}$
25.5	0.25	$t_{2g}\rightarrow\pi_{dppz}$	30.4	0.08	$t_{2g}\rightarrow\pi^*_{dppz}$
27.0	0.22	$\pi\rightarrow\pi^*_{dppz}$	33.1	0.11	$\pi\rightarrow\pi^*$
27.4	0.13	$\pi\rightarrow\pi^*_{dppz}$	34.6	0.50	$\pi\rightarrow\pi^*$
33.2	0.23	$\pi\rightarrow\pi^*_{dppz}$	34.8	0.06	
33.6	1.17	$\pi\rightarrow\pi^*_{dppz}$	35.1	0.16	
33.6	0.11	$\pi\rightarrow\pi^*_{dppz}$	35.2	0.48	
36.6	0.06	mixed	35.3	0.28	
36.6	0.29	$\pi\rightarrow\pi^*_{dppz}$	35.6	0.17	
37.1	0.16	$\pi\rightarrow\pi^*_{dppz}$	35.6	0.10	
37.2	0.14	$t_{2g}\rightarrow\pi_{phen}$	36.6	0.13	
37.3	0.30	$t_{2g}\rightarrow\pi_{phen}$	37.1	0.21	
37.8	0.09	$\pi\rightarrow\pi^*_{dppz}$	37.3	0.20	
38.2	0.05	$\pi\rightarrow\pi^*_{dppz}$	37.9	0.21	
38.8	1.42	$\pi\rightarrow\pi^*_{phen}$	38.2	0.38	
39.0	0.17	$\pi\rightarrow\pi^*_{phen}$	38.9	0.38	
			39.1	1.26	
			39.6	0.31	

changed slightly upon DNA binding. The predicted spectra of free $[Ru(phen)_2dppz]^{2+}$ and $[Ru(phen)_2dppz]^{2+}$ in the field of the two closest base pairs are compared in Table 9. The first band in the observed spectrum has been assigned to $t_{2g}\rightarrow\pi^*$ transitions in both the free complex and the DNA-bonded complex. By inspection of the MOs and the CI eigenvectors, it is clear that the character of the transitions is changed upon DNA binding. In the DNA-bonded complex, the π orbitals are localized to each ligand, in contrast to the free complex, where many π^* orbitals were delocalized on all three ligands. The charge transfer character of most of the $t_{2g}\rightarrow\pi^*$ transitions is increased upon DNA binding.

Summary

We propose a set of parameters for ruthenium, which treats the ruthenium in its Ru^{2+} ionic state rather than the Ru^0 atomic state. The aim is to obtain a set of parameters that can predict both geometry and absorption spectrum of complicated ruthenium organic complexes. We have used known data for two complexes, $[Ru(NH_3)_6]^{2+}$ and $[Ru(bpy)_3]^{2+}$, in the fitting process of the β values for ruthenium. The remaining organometallic complexes have been used as test cases to determine the quality of the parametrization.

In general, the INDO optimized geometries agree well with observed geometries where experimental data are available. Geometry changes upon reduction/oxidation of the metal ion are calculated in less good agreement with observed data. Some of the complexes were also optimized with ab initio calculations, using a relativistic effective core potential for the ruthenium ion. The ab initio calculations predict metal−ligand bond lengths to be much longer than both the INDO model and observed bond lengths. The ligand geometries obtained using the two methods do not differ very much. Furthermore, the agreement between theory and observations is good for the ligand part of the ruthenium complexes.

The general trend for the predicted absorption spectra is that the first MLCT band is too low in energy by about 2000 cm^{-1} for most of the complexes. The $\pi\rightarrow\pi^*$ transitions are calculated in very good agreement with observations. The largest differences between the predicted spectra and the observed spectra are found in cases when the INDO model produces a geometry which agrees less well with the observed geometry (e.g., $[Ru(py)_6]^{2+}$). Some new assignments are proposed. The most important are listed below.

For $[Ru(bpy)_3]^{2+}$, we find a weak MLCT transition in the low-energy region at about the same energy as an experimentally assigned triplet state.

For $[Ru(bpy)_2(py)_2]^{2+}$, we predict the low energy MLCT band to consist of two transitions, one with $t_{2g}\rightarrow$bpy character, and the other having $t_{2g}\rightarrow\pi_{py}$ character. Experimentally, a band and a shoulder are observed at about the same energies, but both are assigned to $t_{2g}\rightarrow\pi_{bpy}$ transitions.

We believe that the proposed parametrization is superior to previously used parameters for ruthenium, as have been demonstrated for the $[Ru(NH_3)_5py]^{2+}$ complex. We have good confidence in the INDO method and think that, with a careful parametrization, as presented here, the method has predictive power. Furthermore, at present, more accurate ab initio methods, where the electron correlation is sufficiently accounted for, such as CASPT2, CCSD, CCSD(T), and MPn methods, cannot be to applied to this type of problems. It still remains a lot of work to investigate the importance of electron correlation and basis set effects on the geometry and absorption spectra of second-row transition metal complexes. In our opinion, at present, INDO-based models are the only methods that can handle this type of complexes.

The effect on the electron structure and absorption spectrum of $[Ru(phen)_2dppz]^{2+}$ of DNA binding was also studied. The ligand-centered MOs were found to be more localized to the individual ligands in the DNA-bonded complex compared with the free complex, where the MOs are delocalized over all ligands. In both the observed and calculated absorption spectra the first band is slightly red shifted, and the band shape is changed upon DNA binding.

Acknowledgment. This work was financed by grants from the Swedish Natural Science Research Council (NFR). The Center for Parallel Computers (PDC) at Stockholm, Sweden, is acknowledged for generous supply of computer time.

Appendix

With the intermediate neglecting of differential overlap (INDO) approximation, the Fock matrix elements are given by

$$F_{\mu\mu} = U_{\mu\mu} + \sum_{\lambda}^{n\in A} P_{\lambda\lambda}\left[(\mu\mu|\lambda\lambda) - \frac{1}{2}(\mu\lambda|\mu\lambda)\right] + \sum_{B}^{N}\left[\sum_{\sigma}^{n\in B} P_{\sigma\sigma} - Z_B\right]\gamma_{AB} \quad \text{(A1)}$$

$$F_{\mu\nu}^{AA} = \frac{1}{2}[P_{\mu\nu}[3(\mu\nu|\mu\nu) - (\mu\mu|\nu\nu)]] \quad \text{(A2)}$$

$$F_{\mu\nu}^{AB} = S_{\mu\nu}\left(\frac{\beta_A + \beta_B}{2}\right) - \frac{1}{2}P_{\mu\nu}\gamma_{AB} \quad \text{(A3)}$$

$$U_{ss} = IP_s - (l-1)F_{ss}^0 - m\left[F_{sp}^0 - \frac{1}{6}G_{sp}^1\right] - n\left[F_{sd}^0 - \frac{1}{10}G_{sd}^2\right] \quad \text{(A4)}$$

$$U_{pp} = IP_p - (m-1)\left[F_{ss}^0 - \frac{2}{25}F_{pp}^2\right] - l\left[F_{sp}^0 - \frac{1}{6}G_{sp}^1\right] - n\left[F_{pd}^0 - \frac{1}{15}G_{pd}^1 - \frac{3}{70}G_{pd}^3\right] \quad \text{(A5)}$$

$$U_{\mu\mu} = \mathrm{IP_d} - (n-1)\left[F^0_{\mathrm{dd}} - \frac{2}{63}(F^2_{\mathrm{dd}} + F^4_{\mathrm{dd}})\right] - l\left[F^0_{\mathrm{sd}} - \frac{1}{10}G^2_{\mathrm{sd}}\right] - m\left[F^0_{\mathrm{pd}} - \frac{1}{15}G^1_{\mathrm{pd}} - \frac{3}{70}G^3_{\mathrm{pd}}\right] \quad \text{(A6)}$$

$$P_{\mathrm{uv}} = \sum_i^{\mathrm{occ}} n_i c_{i,\mu} c_{i,\nu} \quad \text{(A7)}$$

$$(\mu\nu|\lambda\sigma) = \int\int \chi_\mu(1)\chi_\lambda(2)\frac{1}{r_{12}}\chi_\nu(1)\chi_\sigma(2)\,\mathrm{d}\tau_1\,\mathrm{d}\tau_2 \quad \text{(A8)}$$

$$S_{\mu\nu} = \int \chi_\mu \chi_\nu\,\mathrm{d}\tau \quad \text{(A9)}$$

where Z_A is the nuclear charge on atom A, β is an atomic parameter, IP_μ is the ionization potential of atomic orbital μ, F^0_{ss}, F^2_{pp}, $G^1{}_{\mathrm{sp}}$, etc. are atomic Slater−Condon factors, and the indexes l, m, and n are integer numbers corresponding to the atom configuration s^l, p^m, and d^n. F integrals are calculated exactly for the basis set used. The other Slater−Condon factors are taken as semiempirical in the way described in ref 7f.

IC961193N